Analytic formulas for the *D*-mode Robinson instability

Tianlong He,* Weiwei Li, Zhenghe Bai, and Weimin Li

National Synchrotron Radiation Laboratory, University of Science and Technology of China, Hefei, Anhui 230029, China

(Received 1 December 2023; accepted 21 May 2024; published 7 June 2024)

The passive superconducting harmonic cavity (PSHC) scheme is adopted by several existing and future synchrotron light source storage rings, as it has a relatively smaller R/Q and a relatively larger quality factor (Q), which can effectively reduce the beam-loading effect and suppress the mode-one instability. By using a minimum search algorithm to solve the mode-zero Robinson instability equation of uniformly filled rigid bunches, we have revealed that the fundamental mode of PSHC with a large loaded Q possibly triggers the *D*-mode Robinson instability [T. He *et al.*, Mode-zero Robinson instability in the presence of passive superconducting harmonic cavities, Phys. Rev. Accel. Beams **26**, 064403 (2023)]. This instability is a mode-zero coupled bunch instability, with an oscillation frequency close to the PSHC detuning (*D*-mode). Uniquely, it is anti-damped by the radiation damping effect. In this paper, we derive analytical formulas for the frequency and growth rate of the *D*-mode Robinson instability by taking several appropriate approximations. These formulas provide crucial insights for analyzing and understanding the *D*-mode Robinson instability.

DOI: 10.1103/PhysRevAccelBeams.27.064402

I. INTRODUCTION

In the third generation of synchrotron light sources, such as SLS and ELETTRA, passive superconducting harmonic cavities (PSHCs) have been successfully used to elongate the bunch length and thus improve the beam lifetime, with a history of around 20 years. It was reported that SLS and ELETTRA successfully increased the beam lifetime by more than a factor of 2 and 3, respectively [1]. Recently, SSRF has also installed a two-cell PSHC and tested the bunch lengthening performance, successfully doubling the beam lifetime [2]. Their success has to some extent driven more fourth generation synchrotron light sources to adopt the PSHC scheme, such as HALF [3], Diamond-II [4], and Sirius [5], expecting to lengthen the beam by a factor of at least 3 to ensure their high performance of operation.

The loaded quality factor (Q) of PSHC is generally at the level of 1×10^8, which is significantly higher than that of the normal-conducting cavity. In a previous study [6], we revealed that the PSHC fundamental mode impedance may cause a special mode-zero Robinson instability. This instability has an oscillation frequency close to the PSHC detuning (D), so it was called the *D*-mode Robinson instability. It is worth mentioning that this special mode was initially referred to as the cavity mode by Towne and Wang [7], but it was proposed for the main cavity (MC) accelerating mode. This *D*-mode instability driven by PSHC is enhanced with a larger loaded Q value and a smaller radiation damping time. The latter characteristic of the D mode is opposite to any conventional instability that can be mitigated through radiation damping. Generally, the *D*-mode instability will not be triggered unless the PSHC detuning is sufficiently low. That means it will impose a limitation on the bunch lengthening at a relatively low current.

This *D*-mode oscillation was not only observed in simulations [6,8–10] but also likely to be observed in experiments. As early as 20 years ago, in Ref. [1], it was reported for ELETTRA that the voltage feedback loop acting on the PSHC tuning system is opened at about 160 mA because, for lower currents, an instability is then observed causing beam loss. Because $V_h \propto I_0/\Delta f_r$ (with V_h, I_0, and Δf_r denoting the PSHC voltage, beam current, and PSHC detuning, respectively), the voltage feedback will reduce the detuning in an equal proportion as the beam current decreases. It will be shown later that the PSHC detuning of ELETTRA below 160 mA possibly touches the *D*-mode threshold detuning, resulting in beam loss. Another experiment that can be treated as possible evidence of D mode was conducted in SLS and reported at the workshop of HarmonLIP 2022. The threshold detuning for beam loss was measured to be 23.6 kHz at 100 mA [10], which is very close to that of the theoretical *D*-mode threshold detuning [6]. We also noticed that SSRF achieved a bunch lengthening by a factor of about 2.1 for the case of

*htlong@ustc.edu.cn

four uniformly distributed subtrains filling at 200 mA [2], which was still considerably lower than the theoretical near-optimum lengthening ratio. When reducing the PSHC detuning to achieve a larger bunch lengthening ratio, it was observed a beam instability oscillated close to the PSHC detuning and even a beam loss [11]. The above resulting experiments for SSRF are consistent with the prediction based on the D-mode theory, proposed in our previous study [6].

To further prove our viewpoint, we continue this study for the D-mode instability, as a follow-up to our previous study. The possible effects of the MC fundamental mode impedance on the D mode are also considered. It is found that simple analytical formulas for the D-mode oscillation frequency and growth rate can be derived by taking appropriate approximations, and that the MC impedance can enhance the D-mode instability. We will see the limitations imposed by the D mode on the bunch lengthening for the aforementioned three light sources.

The rest of this paper is organized as follows: In Sec. II, we briefly review the mode-zero Robinson instability equation, which is extended to include the MC fundamental mode impedance compared to that in Ref. [6]. In Sec. III, the analytical formulas for the D mode are derived in detail and verified accurately using the Hefei Advanced Light Facility (HALF) storage ring parameters. In Sec. IV, we further apply the analytical formulas to three existing storage rings that employed PSHC. Finally, conclusions and discussions are presented in Sec. V.

II. MODE-ZERO ROBINSON INSTABILITY

In electron storage rings uniformly filled with M equal bunches, the beam instability caused by a narrowband resonator impedance can be described by a well-known equation [12,13]:

$$\Omega^2-\omega_{sg}^2=-i\frac{I_0\alpha_c}{T_0E/e}\sum_{p=-\infty}^{\infty}\{pM\omega_0Z(pM\omega_0)-(pM\omega_0+\mu\omega_0+\Omega)Z(pM\omega_0+\mu\omega_0+\Omega)\},\tag{1}$$

where $\Omega=\Omega_r+i\Omega_i$ is the complex angular oscillation frequency, Ω_r represents the coherent angular frequency, Ω_i is the instability growth rate ($\Omega_i<0$ means damping), i is the imaginary unit, I_0 is the beam average current, α_c is the momentum compaction factor, E is the beam energy, T_0 is the revolution time, ω_0 is the angular revolution frequency, μ is the coupled-bunch mode number taken from 0 to $M-1$, and p is an integer taken from $-\infty$ to $+\infty$, $\omega_{sg}=\sqrt{h\omega_0\alpha_cV_g|\cos(\varphi_g)|/(T_0E/e)}$ is the angular synchronous frequency under beam loading, V_g is the main cavity generator-induced voltage amplitude, φ_g is the corresponding voltage phase, and h is the harmonic number. Note that the ratio h/M is an integer for the uniformly filling case.

It should be noted that Eq. (1) is derived based on the point-like-bunch and linear-wake-force model. Generally, it works well for the case of a narrowband resonator and dipole-oscillation approximation. Here we focus only on the mode-zero ($\mu=0$) coupled bunch instability driven by both the main cavity and the PSHC fundamental modes. The fundamental mode is generally modeled as a single resonator with

$$Z_j(\omega)=\frac{R_j}{1+iQ_j(\frac{\omega_{rj}}{\omega}-\frac{\omega}{\omega_{rj}})},\tag{2}$$

where R_j, Q_j, ω_{rj} are the characteristic parameters of a resonator, representing the loaded shunt impedance, loaded quality factor, and angular resonance frequency, respectively. In the following formulas, for simplicity, we use the subscript $j=1$ and $j=n$ to represent the MC and the PSHC fundamental modes, respectively, and n is the harmonic order of the PSHC.

For the mode-zero instability, the summation of the series on the right-hand side of Eq. (1) is dominated by $pM=\pm nh$ (for $j=n$ mode) and $\pm h$ (for $j=1$ mode). Then Eq. (1) can be simplified as

$$\Omega^2-\omega_{sg}^2+i\frac{I_0\alpha_c}{T_0E/e}\sum_{j=1,n}\{i2jh\omega_0\mathrm{Im}[Z_j(jh\omega_0)]-\omega_{pj}^+Z_j(\omega_p^+)-\omega_{pj}^-Z_j(\omega_{pj}^-)\}=0,\tag{3}$$

where $\omega_{pj}^{\pm}=\pm jh\omega_0+\Omega$. For the MC fundamental mode, we have $\mathrm{Im}[Z_1(h\omega_0))]=-R_1\cos(\psi_1)\sin(\psi_1)$, where ψ_1 is the detuning phase satisfying $\tan(\psi_1)=2Q_1\Delta\omega_{r1}/\omega_{r1}$, and $\Delta\omega_{r1}$ is the angular detuning frequency. In practical operation, the generator-induced voltage will be adjusted to compensate for the beam-induced voltage so that the total cavity voltage is kept constant. Therefore, with the help of phasor diagram, we can know $V_g|\cos(\varphi_g)|+V_{b1}|\sin(\psi_1)|=V_{\mathrm{rf}}|\cos(\varphi_s)|$, where $V_{b1}=2I_0R_1\cos(\psi_1)$ is the beam-induced voltage amplitude, V_{rf} is the main voltage amplitude, and φ_s is the corresponding phase satisfying $V_{\mathrm{rf}}\sin(\varphi_s)=U_0$, U_0 should be considered as the total energy loss per turn, including the radiation loss and the PSHC induced loss. While for the PSHC with a very large loaded quality factor, the energy loss caused by the PSHC is very small and can thus be safely ignored. Besides, we can use the approximation of $\mathrm{Im}[Z_n(nh\omega_0)]\approx-R_n\omega_{rn}/(2Q_n\Delta\omega_{rn})$, with $\Delta\omega_{rn}$ being the angular detuning. Based on the above analysis, Eq. (3) can be further simplified as

$$\Omega^2-\omega_s^2-i\xi\sum_{j=1,n}\{jZ_j(\omega_{pj}^+)-jZ_j(\omega_{pj}^-)\}=0,\tag{4}$$

where we define that

$$\xi = \frac{hI_0\alpha_c\omega_0}{T_0E/e}, \tag{5}$$

$$\omega_s^2 = \omega_{s0}^2 - \frac{n\xi R_n\omega_{rn}}{Q_n\Delta\omega_{rn}}, \tag{6}$$

and

$$\omega_{s0}^2 = \omega_{sg}^2 + \frac{h\omega_0\alpha_c V_{b1}|\sin(\psi_1)|}{T_0E/e} = \frac{\xi V_{\mathrm{rf}}|\cos(\varphi_s)|}{I_0}. \tag{7}$$

Due to the significant role played by radiation damping effect in the D-mode instability [6], it is now time to add it to Eq. (4). Then it gives

$$\Omega^2 + i\frac{2\Omega}{\tau_z} - \omega_s^2 - i\xi\sum_{j=1,n}\{jZ_j(\omega_{pj}^+) - jZ_j(\omega_{pj}^-)\} = 0. \tag{8}$$

The second term on the left-hand side of Eq. (8) represents the radiation damping. If we define a function $g(\Omega)$, whose form is given as follows:

$$g(\Omega) = \Omega^2 + i\frac{2\Omega}{\tau_z} - \omega_s^2 - i\xi\sum_{j=1,n}\{jZ_j(\omega_{pj}^+) - jZ_j(\omega_{pj}^-)\}, \tag{9}$$

the solution of Eq. (8) should meet $g(\Omega) = 0$. Referring to Ref. [6], a search algorithm for the minimum of $|g(\Omega)|$ can also be utilized to find the solution.

It has shown in Ref. [6] that the PSHC with a very large loaded quality factor possibly triggers the D-mode instability. Additionally, by fixing the real part Ω_r and drawing to analyze the dependence of $\mathrm{Re}\{Z(\omega_p^+) - Z(\omega_p^-)\}$ on the imaginary part Ω_i, it was found that the dependence can be fitted by a straight line near $\Omega_i = 0$, that is, it can be expressed as

$$\mathrm{Re}[Z(\omega_p^+) - Z(\omega_p^-)] \approx k\Omega_i + b, \tag{10}$$

where k and b are real coefficients as a function of Ω_r.

Inspired by Eq. (10), we can derive more simplified analytical formulas for the D-mode instability by taking several reasonable approximations. Now we will show the derivation details.

III. DERIVATION OF ANALYTICAL FORMULAS

A. Take the real part

Substitute $\Omega = \Omega_r + i\Omega_i$ into Eq. (9) and take the real part $\mathrm{Re}[g(\Omega)]$, we have

$$\Omega_r^2 - \Omega_i^2 - \frac{2\Omega_i}{\tau_z} - \omega_s^2 + \xi\sum_{j=1,n}\{j\mathrm{Im}[Z_j(\omega_{pj}^+) - Z_j(\omega_{pj}^-)]\} = 0. \tag{11}$$

For the D-mode oscillation, its Ω_r is slightly lower than the angular detuning of PSHC. In general, we can have $\Omega_r \gg \Omega_i$. Thus, the second and the third terms on the left-hand side of Eq. (10) can be ignored, and it gives

$$\Omega_r^2 - \omega_s^2 + \xi\sum_{j=1,n}\{j\mathrm{Im}[Z_j(\omega_{pj}^+) - Z_j(\omega_{pj}^-)]\} \approx 0. \tag{12}$$

Taking $\Omega_r \approx \Delta\omega_{rn}$ and ignoring Ω_i, the terms relevant to the $j = 1$ mode can be transformed as follows:

$$\begin{aligned}&\xi\mathrm{Im}[Z_1(\omega_{p1}^+) - Z_1(\omega_{p1}^-)]\\ &= \xi\mathrm{Im}\left\{\frac{R_1}{1 + i\frac{2Q_1(\Delta\omega_{r1} - \Delta\omega_{rn})}{\omega_{r1}}} - \frac{R_1}{1 - i\frac{2Q_1(\Delta\omega_{r1} + \Delta\omega_{rn})}{\omega_{r1}}}\right\}\\ &= -0.5\xi R_1[\sin(2\psi_-) + \sin(2\psi_+)] = \zeta_1,\end{aligned} \tag{13}$$

where $\psi_\pm$ is determined by

$$\tan(\psi_\pm) = \frac{2Q_1(\Delta\omega_{r1} \pm \Delta\omega_{rn})}{\omega_{r1}}. \tag{14}$$

Under the optimal detuning condition expected to compensate for the beam loading effect, the MC detuning can be expressed as [14]

$$\Delta\omega_{r1} = \frac{h\omega_0 I_0\cos(\varphi_s)}{V_{rf}}\frac{R_1}{Q_1}. \tag{15}$$

It is in general that $\Delta\omega_{r1} < 0$ and $\Delta\omega_{rn} > 0$, so ψ_- is ranged from $-\pi/2$ to 0, and $\psi_- + \psi_+ < 0$.

Let $\Delta\omega_1 = \Delta\omega_{rn} - \Omega_r > 0$ and $\Delta\omega_2 = \Delta\omega_{rn} + \Omega_r \approx 2\Delta\omega_{rn}$, then the terms relevant to the PSHC can be transformed as follows:

$$\begin{aligned}&\xi n\mathrm{Im}[Z_n(\omega_{pn}^+) - Z_n(\omega_{pn}^-)]\\ &= \xi n\mathrm{Im}\left[\frac{R_n}{1 + i\frac{2Q_n\Delta\omega_1}{\omega_{rn}}} - \frac{R_n}{1 - i\frac{2Q_n\Delta\omega_2}{\omega_{rn}}}\right]\\ &\approx -\frac{\xi nR_n}{2Q_n}\left(\frac{\omega_{rn}}{\Delta\omega_1} + \frac{\omega_{rn}}{2\Delta\omega_{rn}}\right).\end{aligned} \tag{16}$$

Substitute Eqs. (13) and (16) into Eq. (12) and take $\Omega_r = \Delta\omega_{rn} - \Delta\omega_1$, we get

$$\Delta\omega_1^3 - 2\Delta\omega_{rn}\Delta\omega_1^2 + \left(\Delta\omega_{rn}^2 + \zeta_1 - \omega_s^2 - \frac{\xi nR_n\omega_{rn}}{4Q_n\Delta\omega_{rn}}\right)\Delta\omega_1 - \frac{\xi n\omega_{rn}R_n}{2Q_n} = 0. \tag{17}$$

Note that Eq. (17) is a cubic equation about $\Delta\omega_1$, which is not difficult to solve. Equation (17) has three solutions, among which only the one closest to zero is desired.

Actually, for the D-mode oscillation, it is in general that $\Delta\omega_1 \ll \Delta\omega_{rn}$. Hence, the first term on the left-hand side of Eq. (17) can be neglected. Then we get

$$\Delta\omega_1^2 - \left(\frac{\Delta\omega_{rn}}{2} + \frac{\zeta_1 - \omega_s^2}{2\Delta\omega_{rn}} - \frac{\xi n R_n \omega_{rn}}{8Q_n\Delta\omega_{rn}^2}\right)\Delta\omega_1 + \frac{\xi n\omega_{rn}R_n}{4\Delta\omega_{rn}Q_n} = 0. \tag{18}$$

Equation (18) is a quadratic equation about $\Delta\omega_1$, which can be solved analytically. If we introduce

$$B_1 = \frac{\Delta\omega_{rn}}{4} + \frac{\zeta_1 - \omega_s^2}{4\Delta\omega_{rn}} - \frac{\xi n R_n\omega_{rn}}{16Q_n\Delta\omega_{rn}^2} \tag{19}$$

and

$$B_2 = \frac{\xi n\omega_{rn}R_n}{4\Delta\omega_{rn}Q_n}, \tag{20}$$

then Eq. (18) has two solutions given as $B_1 \pm \sqrt{B_1^2 - B_2}$. Only the solution closest to zero is required, which is

$$\Delta\omega_1 = B_1 - \sqrt{B_1^2 - B_2}. \tag{21}$$

The D-mode angular oscillation frequency is

$$\Omega_r = \Delta\omega_{rn} - \Delta\omega_1. \tag{22}$$

Note that in the above derivations, we utilized the characteristics of the D-mode instability: (i) the loaded Q-value of PSHC is very large at the level of 10^8 and (ii) $\Delta\omega_1 \ll \Delta\omega_{rn}$.

B. Take the imaginary part

Take the imaginary part $\mathrm{Im}[g(\Omega)]$, it gives

$$2\Omega_r\Omega_i + \frac{2\Omega_r}{\tau_z} - \xi\sum_{j=1,n}\{j\mathrm{Re}[Z_j(\omega_{pj}^+) - Z_j(\omega_{pj}^-)]\} = 0. \tag{23}$$

Also taking $\Omega_r \approx \Delta\omega_{rn}$, then the terms relevant to the MC can be transformed as follows:

$$\begin{aligned}&\xi\mathrm{Re}[Z_1(\omega_{p1}^+) - Z_1(\omega_{p1}^-)]\\ &= \xi\mathrm{Re}\left[\frac{R_1}{1 + i\frac{2Q_1\Delta\omega_-}{\omega_{r1}}} - \frac{R_1}{1 - i\frac{2Q_1\Delta\omega_+}{\omega_{r1}}}\right]\\ &\approx k_1\Omega_i + b_1,\end{aligned} \tag{24}$$

where $\Delta\omega_\pm = \Delta\omega_{r1} \pm \Delta\omega_{rn} \pm i\Omega_i$. To obtain b_1, just let $\Omega_i = 0$, we can have

$$b_1 \approx \xi R_1[\cos^2(\psi_-) - \cos^2(\psi_+)]. \tag{25}$$

To obtain k_1, we should first get the first-order derivation of $\mathrm{Re}[Z_1(\omega_{p1}^+) - Z_1(\omega_{p1}^-)]$ about Ω_i, then let $\Omega_i = 0$, finally, we get

$$\begin{aligned}k_1 &\approx -\xi\frac{2R_1Q_1}{\omega_{r1}}\mathrm{Re}\left[\left(\frac{1}{1 + i\frac{2Q_1\Delta\omega_-}{\omega_{r1}}}\right)^2 - \left(\frac{1}{1 - i\frac{2Q_1\Delta\omega_+}{\omega_{r1}}}\right)^2\right]\\ &= -\xi\frac{2R_1Q_1}{\omega_{r1}}[\cos^2(\psi_-)\cos(2\psi_-) - \cos^2(\psi_+)\cos(2\psi_+)].\end{aligned} \tag{26}$$

Introducing $\Delta\Omega_1 = \Delta\omega_{rn} - \Omega_r - i\Omega_i = \Delta\omega_1 - i\Omega_i$ and $\Delta\Omega_2 = \Delta\omega_{rn} + \Omega_r + i\Omega_i = \Delta\omega_2 + i\Omega_i$, the terms in Eq. (23) relevant to the PSHC can be transformed as follows:

$$\begin{aligned}&\xi n\mathrm{Re}[Z_n(\omega_{pn}^+) - Z_n(\omega_{pn}^-)]\\ &= \xi n\mathrm{Re}\left[\frac{R_n}{1 + i\frac{2Q_n\Delta\Omega_1}{\omega_{rn}}} - \frac{R_n}{1 - i\frac{2Q_n\Delta\Omega_2}{\omega_{rn}}}\right]\\ &\approx k_n\Omega_i + b_n.\end{aligned} \tag{27}$$

Using the same tricks as above for obtaining b_1 and k_1, we can get

$$b_n \approx \xi n\mathrm{Re}\left[\frac{R_n}{1 + i\frac{2Q_n\Delta\omega_1}{\omega_{rn}}}\right] \approx \frac{\xi n R_n\omega_{rn}^2}{4Q_n^2\Delta\omega_1^2}, \tag{28}$$

and

$$k_n \approx -\frac{2\xi nQ_n}{\omega_{rn}R_n}\mathrm{Re}\left[\frac{R_n^2}{(1 + i\frac{2Q_n\Delta\omega_1}{\omega_{rn}})^2}\right] \approx \frac{\xi nR_n\omega_{rn}}{2Q_n\Delta\omega_1^2}. \tag{29}$$

Note in Eqs. (28) and (29) that the terms relevant to $\mathrm{Re}[Z_n(\omega_{pn}^-)]$ are neglected due to $\Delta\omega_2 \gg \Delta\omega_1$, and that $b_n = k_n\omega_{rn}/2Q_n$.

Substitute Eqs. (25), (26), (28), and (29) into Eq. (23), we obtain the D-mode growth rate

$$\Omega_i \approx \frac{b_n + b_1 - 2\Omega_r/\tau_z}{2\Omega_r - k_n - k_1}. \tag{30}$$

C. Verification with the HALF parameters

The Hefei Advanced Light Facility (HALF) [15] is being constructed to be a fourth generation synchrotron light source, with a beam energy of 2.2 GeV and a nominal current of 350 mA. To mitigate the intrabeam scattering and Touschek scattering effects, a PSHC will be adopted to stretch the bunch in the longitudinal direction. Table I summarizes the HALF main parameters as well as both the MC and the PSHC parameters, which will be used for verification of the aforementioned analytical formulas for the D-mode instability.

TABLE I. Main parameters of the HALF storage ring used for the following calculations.

Parameter	Symbol	Value
Beam energy	E	2.2 GeV
Ring circumference	C	479.86 m
Assumed beam current	I_0	40 mA
Longitudinal damping time	τ_z	14 ms
Momentum compaction	α_c	9.4×10^{-5}
Harmonic number	h	800
Energy loss per turn	U_0	400 keV
MC voltage	V_{rf}	1.2 MV
MC normalized shunt impedance	R_1/Q_1	45 Ω
MC loaded quality factor	Q_1	1.14×10^5
MC detuning	Δf_{r1}	−700 Hz
PSHC harmonic order	n	3
PSHC normalized shunt impedance	R_n/Q_n	39 Ω
PSHC loaded quality factor	Q_n	2×10^8
PSHC near-optimum detuning	Δf_{rn}	6 kHz

Note that we chose a relatively low current of 40 mA rather than the nominal current as a study case. This case has already been studied in Ref. [6], mainly to reveal the characteristics of the D-mode instability. In this section, we will prove that the approximate analytical formula is accurate and feasible for the D-mode instability by comparing it with the approach of solving directly the Robinson instability equation.

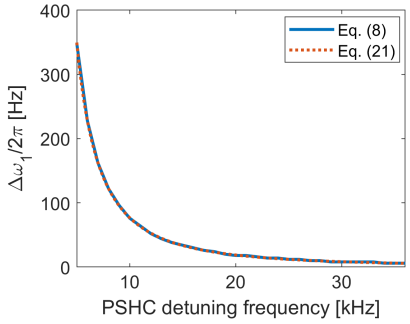

FIG. 1. Frequency deviation $\Delta\omega_1/2\pi$ as functions of the PSHC detuning, obtained by solving directly Eq. (8) and using Eq. (21), respectively.

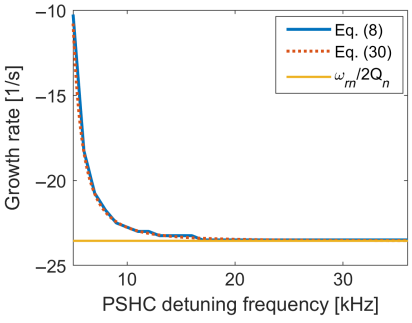

FIG. 2. D-mode growth rate as a function of the PSHC detuning, obtained by solving directly Eq. (8) and using the analytical formula of Eq. (30), respectively.

Figure 1 shows the value of $\Delta\omega_1/2\pi$ (the frequency deviation of the PSHC detuning from the D-mode oscillation angular frequency) as functions of the PSHC detuning ranged from 5 to 36 kHz. Figure 2 shows the corresponding growth rates. It can be seen that the analytical results are in good agreement with those obtained by directly solving the Robinson equation of Eq. (8). Additionally, it can be seen from Fig. 2 that the D-mode damping rate approaches the cavity half bandwidth of $\omega_{rn}/2Q_n$ when increasing the PSHC detuning. This can be understood as a consequence of both $2\Omega_r - k_1 \ll k_n$ and $2\Omega_r/\tau_z - b_1 \ll b_n$. Actually, the above two inequality relationships in general hold true for the case of relatively large detuning of PSHC. In this case, the D-mode growth rate can thus be given as

$$\Omega_i \approx -\frac{b_n}{k_n} = \frac{\omega_{rn}}{2Q_n}. \tag{31}$$

IV. APPLICATION TO REALISTIC STORAGE RINGS

In Sec. III, we obtained the analytical formulas for the D-mode oscillation. In this section, we will use them to analyze the D-mode instability for three realistic storage rings those employed PSHC, including SLS [16], ELETTRA [17,18], and SSRF [19]. Table II summarizes their main parameters.

In practice, the PSHC should be detuned to meet the specific requirements of cavity voltage for reaching the desired bunch lengthening. To facilitate the following discussions, we focus on the near-optimum bunch lengthening condition, with only setting the PSHC voltage amplitude at the optimum lengthening point (due to the nonoptimum phase, it is in general called near optimum). In that case, the PSHC voltage amplitude can be expressed as

$$V_h^{\mathrm{opt}} = k_{\mathrm{opt}} V_{rf} = \frac{F_{\mathrm{opt}} I_0 \omega_{rn} R_n}{\Delta\omega_{rn} Q_n}, \tag{32}$$

where k_{opt} is the corresponding ratio of the PSHC voltage and the MC voltage, and F_{opt} is the corresponding bunch form factor amplitude. Generally, k_{opt} can be pregiven according to the near-optimum lengthening condition, as well as V_h^{opt} and F_{opt}. As a result, the PSHC detuning at the near-optimum lengthening point can be computed by

$$\Delta\omega_{rn}^{\mathrm{opt}} = \frac{F_{\mathrm{opt}} I_0 \omega_{rn} R_n}{V_h^{\mathrm{opt}} Q_n} = \eta \cdot I_0, \tag{33}$$

where η is defined as

$$\eta = \frac{F_{\mathrm{opt}} \omega_{rn} R_n}{V_h^{\mathrm{opt}} Q_n}. \tag{34}$$

TABLE II. Summary of main parameters of SLS, ELETTRA, and SSRF storage rings used for the following calculations and simulations.

Parameters	Unit	SLS	ELETTRA	SSRF
Beam energy	GeV	2.4	2.0	3.5
Circumference	m	288	259.2	432
Harmonic number	⋯	480	432	720
Longitudinal damping time	ms	4.5	8	3
Momentum compaction	⋯	7×10^{-4}	16×10^{-4}	4.2×10^{-4}
rms bunch energy spread	⋯	9.0×10^{-4}	8.0×10^{-4}	11.1×10^{-4}
Energy loss per turn	keV	600	256	1700
MC voltage	MV	2.08	1.7	4.5
MC R_1/Q_1	Ω	312	316	133.5
MC Q_1	⋯	1.333×10^4	1.1×10^4	1.7×10^5
PSHC resonance frequency	MHz	~1500	~1500	~1500
PSHC R_3/Q_3	Ω	88.4	88.4	88
PSHC Q_3	⋯	2×10^8	2×10^8	2×10^8
PSHC V_h^{opt}	kV	660	559	1374
Bunch form factor F_{opt}	⋯	0.883	0.853	0.885
η in Eq. (31)	⋯	1.11×10^6	1.27×10^6	5.34×10^5

The values of V_h^{opt}, F_{opt}, and η are also listed in Table II. Obviously, under the near-optimum PSHC voltage setting, the detuning is proportional to the beam current. In other words, the detuning should be reduced in an equal proportion as the beam current decreases in order to keep the PSHC voltage constant as well as the bunch lengthening. However, the minimum allowable detuning will be limited by the instability. In this paper, we focus on the D-mode threshold detuning, which can be easily computed with the formulas derived in Secs. III B and III C.

It should be noted that the low-level radio-frequency (LLRF) feedback implemented in the main cavities can affect the mode-zero motion, which is, however, not considered in Eq. (8). Equation (8) can be regarded as equivalent to opening the LLRF feedback loop in the presence of MC fundamental mode. To analyze the influence of the LLRF feedback on the D-mode instability and also to validate the analytical results, we will use the STABLE code to conduct multiparticle multibunch tracking simulations [20]. The STABLE is a dedicated longitudinal beam dynamics simulation code that is graphics-processing-unit accelerated. Recently, a proportional-integral (PI) feedback algorithm model has been implemented into the STABLE to achieve a realistic LLRF feedback for the main cavity. The details of the PI model can be found in Appendix A. For a given beam current, we can scan the PSHC detuning in a fixed frequency interval to determine the threshold detuning through observing the oscillations of the mean energy deviation and the PSHC voltage amplitude. In tracking simulations, we only consider the uniform bunch filling. Each bunch is represented by 20,000 macroparticles, and 100,000 turns are tracked.

A. Cases of SLS and ELETTRA with normal-conducting main cavities

Figures 3 and 4 show the resulting threshold detuning frequencies for SLS and ELETTRA, respectively. The legends give the cases of consideration, where "w/ MC" means considering the MC fundamental mode under the open-loop PI feedback, "ideal MC" means treating the MC voltage as an ideal sine wave, the values of k_p and k_i are given corresponding to the proportional and the integral gains, respectively, and $\Delta\omega_{rn}^{\mathrm{opt}}$ is the detuning required for near-optimum bunch lengthening.

First, we can see that for the case of open-loop PI feedback, both the analytical and tracking results are in good agreement, no matter when considering or ignoring the influence of the MC fundamental mode. We can also see that the presence of the MC fundamental mode severely

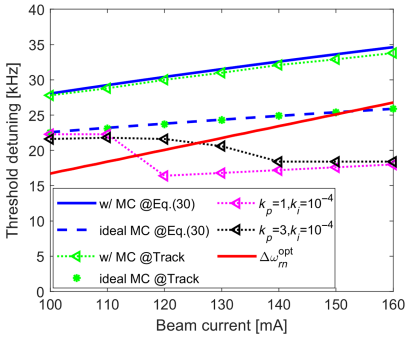

FIG. 3. Threshold detuning as functions of the beam current for SLS, obtained by solving directly Eq. (30) and tracking simulations. For the case of closed-loop PI feedback, the loop delay is set to 1.4 μs. The scanning frequency interval is set to 0.2 kHz, and the threshold detuning is given corresponding to beam loss.

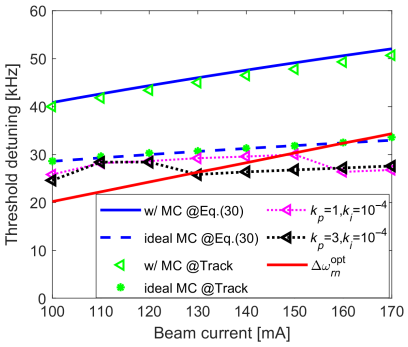

FIG. 4. Threshold detuning as functions of the beam current for ELETTRA, obtained by solving directly Eq. (30) and tracking simulations.

increases the D-mode threshold detuning. This discovery surprised us. How to understand that under the open-loop PI feedback, the presence of the MC fundamental mode enhances the D-mode instability? A reasonable explanation can be given as follows. For the case of normal-conducting main cavities, the term k_1 in Eq. (30) can be given as

$$|k_1| < \xi \frac{4R_1}{\omega_{r1} Q_1} Q_1^2, \tag{35}$$

while for the PSHC, we have

$$k_n \approx \xi \frac{n^2 R_n}{2\omega_{r1} Q_n} \left(\frac{\omega_{r1}}{\Delta\omega_1}\right)^2. \tag{36}$$

Comparing k_n to k_1, we can get

$$k_n/|k_1| > \frac{n^2 R_n Q_1}{8 Q_n R_1} \left(\frac{\omega_{r1}}{\Delta\omega_1 Q_1}\right)^2. \tag{37}$$

For the D-mode oscillation, the $\Delta\omega_1/2\pi$ is generally less than 5 kHz. Using this value and the parameters listed in Table II, we can obtain $k_n/|k_1| > 18$ and 26 for SLS and ELETTRA, respectively. Considering that this is still under conservative estimates, we can thus conclude that compared to k_n, k_1 can be safely neglected when using Eq. (30) for the D mode. Finally, for the cases of SLS and ELETTRA, the D-mode growth rate can be given as

$$\Omega_i \approx \frac{b_n + b_1 - 2\Omega_r/\tau_z}{2\Omega_r - k_n}. \tag{38}$$

Note that both k_n and b_n are positive, and $b_1 < 0$ due to the fact that $\psi_- + \psi_+ < 0$.

To facilitate the subsequent analysis, Eq. (38) should be changed as

$$\Omega_i = \frac{1}{\tau_z} \frac{k_n \tau_z \omega_{rn}/2Q_n - (2\Omega_r - b_1\tau_z)}{2\Omega_r - k_n}. \tag{39}$$

Considering the radiation damping time realistically ranged from 1 to 20 ms and the PSHC loaded Q value generally larger than 1×10^8, we can have $\tau_z \omega_{rn}/2Q_n < 1$. Consequently, as the PSHC detuning decreases, the numerator approaches zero faster than the denominator. Therefore, for the D mode of interest, it is in general that $2\Omega_r < k_n$. In other words, the D mode is naturally damped by the PSHC fundamental mode impedance, while it is antidamped by the radiation-damping effect and is enhanced by the MC fundamental mode impedance. This enhancement is observed to be significant because b_1 is not small compared to the radiation damping term.

For the case of closed-loop PI feedback, as can be seen from Figs. 3 and 4, the feedback can significantly reduce the threshold detuing of beam loss, which is even lower than that of only considering PSHC fundamental mode impedance. It should be noted that the threshold detuning of beam loss may not only be limited by the D mode, but in some cases, it may also be limited by other types of instability, such as the $S-D$ mode coupling [6]. The setting of feedback parameters has a significant impact on the specific beam instability behavior. Nevertheless, based on the resulting threshold, we can conclude that the D-mode instability can be suppressed effectively with the PI feedback on the main cavities. It should be pointed out that theoretical analysis of the specific effects of PI feedback on beam instabilities is complex and beyond the scope of this paper. Nevertheless, a qualitative understanding can be given as follows.

We noticed that the loaded Q values of the SLS and ELETTRA main cavities are approximately 10^4, corresponding to a bandwidth of approximately 25 kHz; while the PSHC detuning is close to or even lower than this bandwidth. Therefore, the D-mode oscillation will also excite the MC voltage oscillation. As we know that the PI feedback aims at stabilizing the MC voltage, which can naturally help to suppress the D-mode oscillation. In addition, when the PI feedback is on, we should consider the closed-loop cavity impedance, which is the cavity impedance seen by the beam in the presence of feedback [21]. In that case, the term of b_1 in Eq. (30) can be reduced, and the amount of reduction largely depends on the feedback parameters, especially the value of k_p. From this point, the PI feedback can reduce the enhancement of D-mode instability caused by the MC impedance.

B. Case of SSRF with superconducting main cavities

Figure 5 shows the D-mode threshold detuning for SSRF as functions of the beam current ranged from 100 to 300 mA. It can be seen that the resulting analytical and tracking threshold detunings are in good agreement for the case of open-loop PI feedback. In addition, it can be seen that the presence of MC impedance slightly increases the threshold detuning, which is considerably different from those shown in Figs. 3 and 4. This can be attributed to the

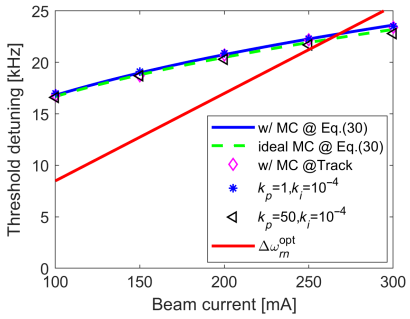

FIG. 5. Threshold detuning as functions of the beam current for SSRF, obtained by solving directly Eq. (30) and tracking simulations.

fact that the term of b_1 in Eq. (30) is relatively small compared to the radiation damping term.

For the case of closed-loop PI feedback, it can be seen that the PI feedback affects slightly the D-mode threshold detuning, even if the proportional gain k_p changes a lot. Similar to the analysis for the case of normal-conducting main cavities, we can also understand that from the perspective of cavity bandwidth. The MC loaded Q value of SSRF is approximately 1.7×10^5, corresponding to a bandwidth of less than 3 kHz; while the PSHC detuning is larger than 15 kHz, which is largely beyond the bandwidth. Therefore, the D-mode oscillation driven by the PSHC is almost transparent to the MC voltage variation, and in turn, the PI feedback used to stabilize the MC voltage will hardly affect the D-mode motion.

We can see that there is an intersection between the near-optimum lengthening detuning line and the D-mode threshold detuning line. The intersection point is at the beam current of approximately 262 mA. For the case of beam current lower than that point, it is clear that the D mode will impose a limitation on the bunch lengthening, resulting in the failure to reach the near-optimum bunch lengthening.

V. CONCLUSION AND DISCUSSION

As a follow-up to our previous research [6], we have made further efforts in this paper to derive simpler analytical formulas for analyzing the D-mode instability. The contributions of this paper can be summarized as follows: (i) Based on the characteristic of D mode that it has a small frequency deviation from the PSHC detuning, appropriate approximations are taken to derive analytical formulas for calculating the D-mode frequency and growth rate, which makes its dependency on relevant parameters more intuitive. (ii) For the case of a relatively large detuning, the D-mode has a negative growth rate (is damped) whose absolute value approaches the PSHC half bandwidth. This has not been discovered in our previous study. (iii) The analytical formulas can be used more easily to compute the threshold detuning, and the results are in good agreement with those obtained by tracking simulations, which holds at least for three realistic storage rings. Based on the analytical formulas, it has revealed that the MC fundamental mode impedance can enhance the D mode significantly (or slightly), depending on whether the cavity is normal-conducting (or superconducting). (iv) Combined with tracking simulations, it has shown that the PI feedback can suppress the D mode effectively for the case of normal-conducting main cavities; while for the case of superconducting main cavities, it affects hardly the D mode. This difference can be attributed to the different cavity bandwidth. (v) It can be seen from the derivation process for the D-mode growth rate formula of Eq. (30) that the real part of the PSHC fundamental mode impedance determines the value of b_n; while the imaginary part determines the value of k_n, which is positive and has a so large value that $2\Omega_r - k_n < 0$. The latter is the main factor of determining the D-mode characteristic of being antidamped by the radiation damping effect. Therefore, the imaginary part plays a more crucial role in the D-mode motion.

It should be pointed out that the derivation method demonstrated in this paper is not limited to analyzing the D-mode instability but can also be extended to mode 1 instability [22,23]. However, this part is beyond the scope of this paper and will be discussed elsewhere.

Finally, it should be emphasized that the D-mode instability needs to be considered only when the PSHC is operated in bunch lengthening mode. For the case of bunch shortening, we can directly solve the mode-zero Robinson instability equation, and of course, we can also derive analytical formulas for analyzing the D-mode instability. In that case, it can be found that the D mode is always stable. The relevant derivations are shown in Appendix B for the reader's reference.

ACKNOWLEDGMENTS

One of the authors greatly appreciates the valuable discussions with Alexander Wu Chao and also his insightful suggestions. We thank Hongtao Hou at SSRF for friendly discussions. This research was supported by the National Natural Science Foundation of China (Grants No. 12105284, No. 12375324, and No. 12341501).

APPENDIX A: PI FEEDBACK IMPLEMENTED IN THE STABLE CODE

The STABLE code can be available via the link [24]. A realistic PI feedback has already been implemented in the STABLE to stabilize the MC voltage. The whole procedure of the PI feedback, as shown in Fig. 6, mainly consists of three parts:

(i) To compute the error current phasor $\Delta\tilde{V}/R_L$, where R_L is the loaded shunt impedance, and $\Delta\tilde{V}$ is the error voltage phasor between the desired voltage phasor $\tilde{V}_{\rm set}$ and the measured voltage phasor $\langle\tilde{V}_c\rangle$. The measured voltage

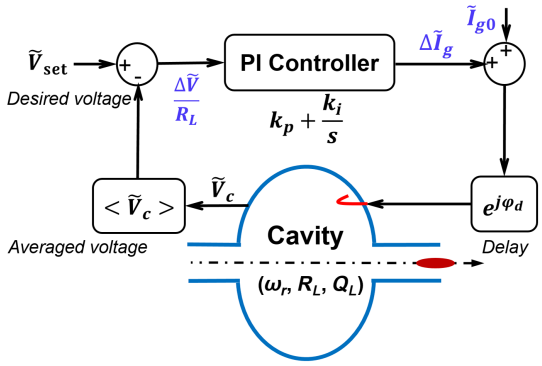

FIG. 6. Implementation of the PI feedback loop in the STABLE tracking code. The PI controller is represented by the transfer function of $k_p + k_i/s$, where k_p and k_i are the proportional and integral gains, respectively. The cavity voltage phasor $\tilde{V}_c$ is driven by both the generator current and the beam current.

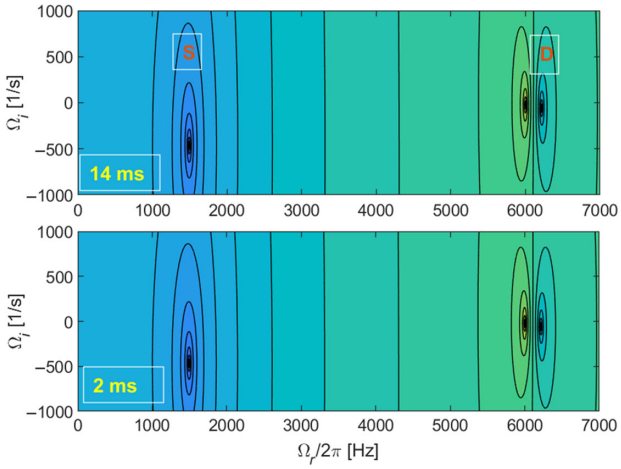

FIG. 7. Contour map of $\log(|g(\Omega)|)$ for the case of detuning of −6 kHz. The top and the bottom correspond to the cases of damping times of 14 and 2 ms, respectively. The left local minimum corresponds the synchronous oscillation (labeled as S), while the right one to the PSHC detuning (labeled as D).

phasor is assumed to be the averaged voltage phasor among a certain number of buckets (tens of buckets).

(ii) Input the error current phasor to the PI controller, then output the corrected generator current phasor $\Delta\tilde{I}_g$.

(iii) To update the generator current phasor with $\tilde{I}_{g0} + \Delta\tilde{I}_g$, where $\tilde{I}_{g0}$ is the initialized generator current phasor. After a delay of a certain number of buckets ($1 - 2$ μs), this updated generator current starts acting on the cavity voltage.

APPENDIX B: ANALYTICAL FORMULAS FOR THE D MODE IN THE CASE OF BUNCH SHORTENING

For the case of PSHC operated in bunch shortening mode, the search algorithm for minimum can be also used directly to solve the mode-zero Robinson instability equation. We still take the HALF storage ring as an example. Using the parameters listed in Table I and assuming the detuning frequency of −6 kHz, the resulting 2D contour maps of $\log(|g(\Omega)|)$ are shown in Fig. 7. It can be seen that for both cases of $\tau_z = 14$ ms and $\tau_z = 2$ ms, the D-mode frequency is slightly larger than the detuning of PSHC, which is opposite to the case of bunch lengthening. This feature can be utilized to derive the oscillation frequency and growth rate formulas for the D mode.

Take the real part of Eq. (8) and ignore unimportant terms, it also gives

$$\Omega_r^2 - \omega_s^2 + \xi \sum_{j=1,n} \{j\mathrm{Im}[Z_j(\omega_{pj}^+) - Z_j(\omega_{pj}^-)]\} \approx 0. \quad \text{(B1)}$$

Here, we set $\Delta\omega_{rn} = nh\omega_0 - \omega_{rn} > 0$, and it is already known that Ω_r is slightly higher than $\Delta\omega_{rn}$. If introduce $\Delta\omega_1 = \Omega_r + \Delta\omega_{rn}$ and $\Delta\omega_2 = \Omega_r - \Delta\omega_{rn}$, then the terms related to the PSHC can be transformed as follows:

$$\begin{aligned}
&\xi n\mathrm{Im}[Z_n(\omega_{pn}^+) - Z_n(\omega_{pn}^-)] \\
&= \xi n\mathrm{Im}\left[\frac{R_n}{1 - i\frac{2Q_n\Delta\omega_1}{\omega_{rn}}} - \frac{R_n}{1 - i\frac{2Q_n\Delta\omega_2}{\omega_{rn}}}\right] \\
&\approx -\frac{\xi n R_n}{2Q_n}\left(\frac{\omega_{rn}}{\Delta\omega_2} - \frac{\omega_{rn}}{2\Delta\omega_{rn}}\right). \quad \text{(B2)}
\end{aligned}$$

For the terms relevant to the MC, we can obtain the same equation as Eq. (13). Substitute Eqs. (B2) and (13) into Eq. (B1) and take appropriate simplifications, a quadratic equation about $\Delta\omega_2$ is finally obtained

$$\begin{aligned}
&\Delta\omega_2^2 + \left(\frac{\Delta\omega_{rn}}{2} + \frac{\zeta_1 - \omega_s^2}{2\Delta\omega_{rn}} + \frac{\xi n R_n \omega_{rn}}{8Q_n\Delta\omega_{rn}^2}\right)\Delta\omega_2 \\
&- \frac{\xi n\omega_{rn}R_n}{4\Delta\omega_{rn}Q_n} = 0. \quad \text{(B3)}
\end{aligned}$$

If we introduce

$$B_3 = \frac{\Delta\omega_{rn}}{4} + \frac{\zeta_1 - \omega_s^2}{4\Delta\omega_{rn}} + \frac{\xi n R_n \omega_{rn}}{16Q_n\Delta\omega_{rn}^2}, \quad \text{(B4)}$$

and still use Eq. (20) of B_2, it is easy to know Eq. (B3) has two solutions of $-B_3 \pm \sqrt{B_3^2 + B_2}$, where only the one closest to zero is required. Therefore, we get

$$\Delta\omega_2 = -B_3 + \sqrt{B_3^2 + B_2}. \quad \text{(B5)}$$

The D-mode angular frequency can be written as

$$\Omega_r = \Delta\omega_r + \Delta\omega_2. \quad \text{(B6)}$$

Taking the same derivations as introduced in Sec. III B, we can also obtain the D-mode growth rate for the case of bunch shortening:

$$\Omega_i \approx \frac{b_n + b_1 - 2\Omega_r/\tau_z}{2\Omega_r - k_n - k_1}, \tag{B7}$$

where b_1 and k_1 can also be given by Eqs. (25) and (26), respectively, since we set $\Delta\omega_{rn} = nh\omega_0 - \omega_{rn} > 0$. In addition, b_n and k_n are given, respectively, as follows:

$$b_n \approx -\frac{\xi n R_n \omega_{rn}^2}{4Q_n^2\Delta\omega_2^2}, \tag{B8}$$

and

$$k_n \approx -\frac{\xi n R_n \omega_{rn}}{2Q_n\Delta\omega_2^2}. \tag{B9}$$

It should be noted that all of b_1, b_n, and k_n are always less than zero. Additionally, it is in general that $|k_1| \ll |k_n|$. Consequently, the denominator in Eq. (B7) is always larger than zero. It indicates that for the case of bunch shortening, the D-mode oscillation is always damped, which is ensured by the PSHC and the MC fundamental modes, as well as the radiation damping effect.

[1] M. Pedrozzi, W. Gloor, A. Anghel, M. Svandrlik, G. Penco, P. Craievich, A. Fabris, C. Pasotti, E. Chiaveri, R. Losito, S. Marque, O. Aberle, P. Marchand, P. Bosland, S. Chel, P. Brédy, and G. Devanz, First operation results of the 3rd harmonic super conducting cavities in SLS and ELETTRA, in *Proceedings of the 20th Particle Accelerator Conference, PAC-2003, Portland, OR* (IEEE, New York, 2003), pp. 878–880, MPPB024.

[2] Z. G. Zhang, Y. B. Zhao, K. Xu, X. Zheng, Q. Chang, S. J. Zhao, Z. Y. Ma, H. R. Jiang, W. F. Yang, X. F. Huang, Y. Wang, J. Shi, and H. T. Hou, Low level radio frequency controller for superconducting third harmonic cavity at SSRF, Nucl. Tech. **45**, 120101 (2022).

[3] Y. Wei, J. Pang, B. Du, D. Jia, S. Zhang, and G. Feng, Design of a passive superconducting harmonic cavity for HALF storage ring, in *Proceedings of the 13th International Particle Accelerator Conference, IPAC-2022, Bangkok, Thailand*, (JACoW, Geneva, Switzerland, 2022), pp. 1378–1380, TUPOTK065.

[4] Diamond-II: Technical Design Report, Diamond Light Source Ltd., 2022, https://www.diamond.ac.uk/Home/News/LatestNews/2022/14-10-22.html.

[5] I. C. Almeida, A. P. B. Lima, and M. H. Wallner, Third harmonic superconducting cavity for bunch lengthening and beam lifetime increase of Siruis synchrotron light source, in *Proceedings of the 20th International Conference on RF Superconductivity. SRF-2021, East Lansing, MI* (JACoW, Geneva, Switzerland, 2021), pp. 37–41, SUPCAV011.

[6] T. L. He, W. W. Li, Z. H. Bai, and W. M. Li, Mode-zero Robinson instability in the presence of passive superconducting harmonic cavities, Phys. Rev. Accel. Beams **26**, 064403 (2023).

[7] N. Towne and J.-M. Wang, Spectrum of single bunch longitudinal dipole modes, Phys. Rev. E **57**, 3461 (1998).

[8] N. Carmignani, J. Jacob, B. Nash, and S. White, Harmonic rf system for the ESRF EBS, in *Proceedings of the International Particle Accelerator Conference, IPAC-2017, Copenhagen, Denmark* (JACoW, Geneva, Switzerland, 2017), pp. 3684–3687, THPAB003.

[9] A. Gamelin, Harmonic cavity studies for the SOLEIL Upgrade, in *Proceedings of iFAST Workshop 2022 Beam Diagnostics and Dynamics in Ultra-low Emittance Rings, Virtual Workshop* (2022), https://indico.scc.kit.edu/event/2592/sessions/2579/attachments/5006/7591/Slides_3-1_Gamelin.pdf.

[10] L. Stingelin, Tracking simulations and tests results in SLS with Super-3HC, in *Proceedings of HarmonLIP 2022, Lund, MAX IV* (2022), https://indico.maxiv.lu.se/event/5098/contributions/6755/attachments/1171/2310/20221001-HarmonLIPworkshopV2.pptx.

[11] H. T. Hou (private communication).

[12] A. W. Chao, *Physics of Collective Beam Instabilities in High Energy Accelerators* (Wiley, New York, 1993), p. 162.

[13] K. Y. Ng, *Physics of Intensity Dependent Beam Instabilities* (World Scientific Publishing, Singapore, 2006), p. 313.

[14] H. Padamsee, J. Knobloch, and T. Hays, *RF Superconductivity for Accelerators* (Wiley, New York, 1998).

[15] Z. H. Bai, G. Feng, T. He, W. Li, W. Li, G. Liu, J. Tang, L. Wang, P. Yang, and S. Zhang, Progress on the storage ring physics design of Hefei Advanced Light Facility (HALF), in *Proceedings of the 14th International Particle Accelerator Conference, IPAC-2023, Venice, Italy* (JACoW, Geneva, Switzerland, 2023), pp. 1075–1078, MOPM038.

[16] SLS 2.0 Storage Ring Technical Design Report, PSI Bericht, Switzerland, Report No. 21-02 PSI, 2021.

[17] ELETTRA 2.0 Technical Design Report, Elettra – Sincrotrone Trieste, internal document, Report No. ST/M-21/01, 2021.

[18] G. Penco and M. Svandrlik, Experimental studies on transient beam loading effects in the presence of a superconducting third harmonic cavity, Phys. Rev. ST Accel. Beams **9**, 044401 (2006).

[19] X. Wu, S. Q. Tian, X. Z. Liu, W. Z. Zhang, and Z. T. Zhao, Design and commissioning of the new SSRF storage ring lattice with asymmetric optics, Nucl. Instrum. Methods Phys. Res., Sect. A **1025**, 166098 (2022).

[20] T. L. He and Z. H. Bai, Graphics-processing-unit-accelerated simulation for longitudinal beam dynamics of arbitrary bunch trains in electron storage rings, Phys. Rev. Accel. Beams **24**, 104401 (2021).

[21] P. Baudrenghien and T. Mastoridis, Fundamental cavity impedance and longitudinal coupled-bunch instabilities at the High Luminosity Large Hadron Collider, Phys. Rev. Accel. Beams **20**, 011004 (2017).

[22] M. Venturini, Passive higher-harmonic rf cavities with general settings and multibunch instabilities in electron storage rings, Phys. Rev. Accel. Beams **21**, 114404 (2018).

[23] T. He, W. Li, Z. Bai, and L. Wang, Periodic transient beam loading effect with passive harmonic cavities in electron storage rings, Phys. Rev. Accel. Beams **25**, 024401 (2022).

[24] https://github.com/hetianlong-afk/STABLE